Published in final edited form as:
Nature. 2014 August 7; 512(7512): 69–73. doi:10.1038/nature13322.

Negative regulation of the NLRP3 inflammasome by A20 protects against arthritis

Lieselotte Vande Walle[1,2], **Nina Van Opdenbosch**[1,2], **Peggy Jacques**[3], **Amelie Fossoul**[1,2], **Eveline Verheugen**[3], **Peter Vogel**[4], **Rudi Beyaert**[5,6], **Dirk Elewaut**[3], **Thirumala-Devi Kanneganti**[4], **Geert van Loo**[#5,6], and **Mohamed Lamkanfi**[#1,2]

[1]Department of Medical Protein Research, VIB, Ghent, B-9000, Belgium

[2]Department of Biochemistry, Ghent University, Ghent, B-9000, Belgium

[3]Department of Rheumatology, Ghent University, B-9000 Ghent, Belgium

[4]Department of Immunology, St. Jude Children's Research Hospital, Memphis, TN 38105, USA

[5]Inflammation Research Center, VIB, Ghent, B-9052, Belgium

[6]Department of Biomedical Molecular Biology, Ghent University, B-9052 Ghent, Belgium

[#] These authors contributed equally to this work.

Abstract

Rheumatoid arthritis (RA) is a chronic autoinflammatory disease that affects 1-2% of the world population and is characterized by widespread joint inflammation. IL-1 is an important mediator of cartilage destruction in rheumatic diseases[1], but our understanding of the upstream mechanisms leading to IL-1β production in rheumatoid arthritis is limited by the absence of suitable RA mouse models in which inflammasomes contribute to pathology. Myeloid-cell-specific deletion of the RA-susceptibility gene *A20/TNFAIP3* in mice (*A20*$^{myel\text{-}KO}$ mice) triggers a spontaneous erosive polyarthritis that resembles RA in patients[2]. Notably, RA in *A20*$^{myel\text{-}KO}$ mice was not rescued by tumor necrosis factor receptor 1 (TNF-R1) deletion, but we showed it to crucially rely on interleukin-1 receptor (IL-1R) signaling. Macrophages lacking A20 had increased basal and LPS-induced expression levels of the inflammasome adaptor Nlrp3 and proIL-1β. As a result, A20-deficiency in macrophages significantly enhanced Nlrp3 inflammasome-mediated caspase-1 activation, pyroptosis and IL-1β secretion by soluble and crystalline Nlrp3 stimuli. In contrast, activation of the Nlrc4 and AIM2 inflammasomes was not altered. Importantly, increased Nlrp3 inflammasome activation contributed to RA pathology *in vivo*, because deletion of Nlrp3 and caspase-1 markedly protected against RA-associated inflammation and cartilage destruction in

[*]Correspondence and requests for materials should be addressed to: Mohamed Lamkanfi, Department of Medical Protein Research, VIB, Albert Baertsoenkaai 3, B-9000 Ghent, Belgium, Tel: +32 9 264 9341; Fax: +32 9264 9490; mohamed.lamkanfi@vib-ugent.be.

Author contributions: L.V.W., G.V.L., M.L. designed the study; L.V.W., N.V., A.F., P.J., E.V. and P.V. performed experiments; L.V.W., N.V., P.J., P.V., G.V.L., R.B., D.E., T.-D.K. and M.L. analyzed data and wrote the manuscript; T.-D.K. provided essential reagents and scientific insight; M.L. oversaw the project.

The authors declare no competing financial interests.

Europe PMC Funders Author Manuscripts

A20$^{myel\text{-}KO}$ mice. These results reveal A20 as a novel negative regulator of Nlrp3 inflammasome activation, and describe *A20*$^{myel\text{-}KO}$ mice as the first experimental model to study the role of inflammasomes in RA pathology.

Keywords

inflammasome; Nlrp3; A20; caspase-1; IL1R1

A20 was deleted in myeloid cells by crossing *A20*$^{flox/flox}$ mice into Lysosyme M (LysM)-Cre recombinase-expressing mice. Unlike wild-type macrophages, *A20*$^{myel\text{-}KO}$ macrophages failed to induce A20 mRNA and protein expression in response to the TLR4 ligand LPS (Fig. 1a, b), demonstrating the effectiveness of LysM-driven deletion of A20 in myeloid cells. Arthritis development in *A20*$^{myel\text{-}KO}$ mice was shown to be TNFR1-independent, whereas deletion of MyD88 markedly protected against RA pathology[2]. As this signaling adaptor operates downstream of both TLRs and IL-1R, we crossed *IL1R1*$^{-/-}$ mice into *A20*$^{myel\text{-}KO}$ mice to assess the contribution of IL-1 signaling to arthritis pathogenesis. As expected, wild-type mice (*A20*$^{flox/flox}$*IL1R1*$^{+/+}$) did not develop arthritis, whereas *A20*$^{myel\text{-}KO}$ mice spontaneously developed an arthritic phenotype (Fig. 1c). The incidence of *A20*$^{myel\text{-}KO}$ mice developing arthritis was 100% (Fig. 1d). In sharp contrast, *A20*$^{myel\text{-}KO}$*IL1R1*$^{-/-}$ mice were virtually devoid of clinical signs of arthritis (Fig. 1c, d). In agreement, clinical scoring of disease severity confirmed *A20*$^{myel\text{-}KO}$*IL1R1*$^{+/+}$ mice to develop severe arthritic disease (high clinical score) whereas *A20*$^{myel\text{-}KO}$*IL1R1*$^{-/-}$mice were markedly protected (clinical score 0). *A20*$^{myel\text{-}KO}$ littermates that were heterozygous for IL1R1 expression showed an intermediate arthritic phenotype between those of *A20*$^{myel\text{-}KO}$*IL1R1*$^{+/+}$ and *A20*$^{myel\text{-}KO}$*IL1R1*$^{-/-}$ mice (Fig. 1d, e). These clinical assessments were supported by a histological examination of representative ankle joints. Hematoxylin and eosin-stained tissue sections of diseased *A20*$^{myel\text{-}KO}$*IL1R1*$^{+/-}$ mice showed significant synovial and periarticular inflammation and high levels of infiltrated mononuclear cells, which was associated with extensive cartilage and bone destruction (Fig. 1f). In marked contrast, ankle joints of *A20*$^{myel\text{-}KO}$*IL1R1*$^{-/-}$ littermates were strongly protected from arthritic histopathology and contained significantly reduced numbers of infiltrating inflammatory cells (Fig. 1f). Semi-quantitative scoring of these histological parameters confirmed that the severity of arthritis was substantially lower in *A20*$^{myel\text{-}KO}$*IL1R1*$^{-/-}$ mice relative to *A20*$^{myel\text{-}KO}$*IL1R1*$^{+/-}$ littermates (Fig. 1g and Extended Data Table 1). These results demonstrate that IL-1 production is detrimental for arthritis pathogenesis in mice with a myeloid cell-restricted deletion in *A20*.

Macrophages are a prime source of proIL-1β, and generally depend on caspase-1 for maturation and secretion of the biologically active cytokine. Caspase-1 is produced as a cytosolic zymogen, the activation of which is controlled by different inflammasomes[3]. To study the role of A20 in inflammasome signaling, we assessed caspase-1 processing in bone marrow-derived macrophages (BMDMs) of wild-type and *A20*$^{myel\text{-}KO}$ mice. Notably, caspase-1 activation was substantially increased in LPS-primed *A20*$^{myel\text{-}KO}$ macrophages that were treated with soluble (ATP and nigericin) or crystalline (silica) stimuli of the Nlrp3 inflammasome compared to wild-type BMDMs (Fig. 2a). Concurrently, the levels of

Europe PMC Funders Author Manuscripts

secreted IL-1β in the culture medium of ATP- and nigericin-treated *A20*$^{myel\text{-}KO}$ macrophages were about twice those of wild-type cells, and silica triggered nearly four times higher levels of secreted IL-1β (Fig. 2b). Enhanced caspase-1 autoprocessing (Fig. 2c, d) and IL-1β secretion (Fig. 2e, f) by the Nlrp3 inflammasome was evident within 10 minutes after ATP or nigericin addition, and continued to increase in a time-dependent fashion. Similarly, the induction of caspase-1-dependent pyroptosis was enhanced in *A20*$^{myel\text{-}KO}$ macrophages (Fig. 2g, h). Despite their hypersensitivity for Nlrp3 inflammasome activation, *A20*$^{myel\text{-}KO}$ macrophages failed to process caspase-1, and secrete IL-1β and IL-18 when treated with LPS, ATP or nigericin alone (Extended Data figure 1). The increased responsiveness of *A20*$^{myel\text{-}KO}$ macrophages towards inflammasome activation was restricted to the Nlrp3 inflammasome because caspase-1 processing and pyroptotic cell death by the Nlrc4 inflammasome were similarly induced in wild-type and *A20*$^{myel\text{-}KO}$ macrophages that had been infected with *Salmonella* Typhimurium (*S.* Typhimurium) (Fig. 2i, j). Similarly, stimulation of the AIM2 inflammasome with cytosolic dsDNA did not result in differential levels of caspase-1 processing and pyroptosis induction in wild-type and *A20*$^{myel\text{-}KO}$ macrophages (Fig. 2k, l). It is worth noting, however, that despite normal caspase-1 activation and pyroptosis levels in response to *S.* Typhimurium infection and dsDNA transfection, secretion of IL-1β in response to these treatments was consistently higher in *A20*$^{myel\text{-}KO}$ macrophages compared to wild-type controls (Fig. 2m, n), which could be explained by increased induction of proIL-1β mRNA in *A20*$^{myel\text{-}KO}$ macrophages (data not shown). Together, these results demonstrate that A20 negatively regulates activation of caspase-1 by the Nlrp3 inflammasome, but not by the Nlrc4 and AIM2 inflammasomes.

Activation of the Nlrp3 inflammasome in wild-type macrophages is tightly regulated at different levels. A priming signal (referred to as step 1 and usually provided by TLRs) upregulates Nlrp3 expression levels along with the inflammasome substrate proIL-1β via the pro-inflammatory transcription factor NF-κB[4]. A20 negatively regulates LPS-induced NF-κB activation (refs.[5-8] and Extended Data figure 2a), which also was reflected in increased secretion of the NF-κB-dependent cytokines IL-6 and TNF in *A20*$^{myel\text{-}KO}$ macrophages (Extended Data figure 2b, c). We further showed A20-deficiency to markedly enhance LPS-induced mRNA expression levels of Nlrp3 (Fig. 3a) and proIL-1β (Fig. 3b). In contrast, LPS-induced transcript levels of caspase-1 and the inflammasome adaptor ASC were respectively mildly upregulated and normal in *A20*$^{myel\text{-}KO}$ macrophages (Extended Data figure 3a, b). Analysis of protein expression levels confirmed Nlrp3 and proIL-1β to be significantly higher in LPS-primed *A20*$^{myel\text{-}KO}$ macrophages compared to wild-type cells, whereas caspase-1 and ASC were not differentially modulated in the two genotypes (Fig. 3c).

TLR stimulation during brief time intervals (10 minutes or less) was recently shown to license activation of the Nlrp3 inflammasome independently of new protein synthesis[9-12]. Rapid Nlrp3 inflammasome activation resulted in procaspase-1 processing and secretion of pre-synthesized proIL-18 in the absence of the NF-κB dependent cytokines IL-1β, TNF and IL-6[9-11]. To address whether A20 modulated rapid Nlrp3 inflammasome activation, cells were exposed to ATP or nigericin after being primed with LPS for 10 minutes. As reported[9-12], wild-type BMDMs activated caspase-1 (Fig. 3d) and secreted significant

amounts of IL-18, but not IL-1β, TNF or IL-6 (Fig. 3e). Moreover, we noted Nlrp3 protein levels were lowered after stimulation in both wild-type and *A20*$^{myel\text{-}KO}$ macrophages (Fig. 3d), supporting the notion that acute Nlrp3 inflammasome activation occurred independently of LPS-induced new protein synthesis. Both caspase-1 processing and IL-18 secretion were markedly increased in *A20*$^{myel\text{-}KO}$ macrophages in the absence of substantial IL-1β, TNF and IL-6 secretion (Fig. 3d, e). This was likely due to increased basal expression of Nlrp3 and proIL-18 in these cells (Fig. 3a, d). In agreement, basal mRNA levels of Nlrp3, proIL-1β and proIL-18 were increased in untreated A20$^{myel\text{-}KO}$ macrophages (Fig. 3a, b and Extended Data figure 3c). Together, these results suggest that A20 negatively regulates Nlrp3 inflammasome signaling by suppressing NF-κB-dependent production of Nlrp3 and the inflammasome substrates proIL-1β and proIL-18. In agreement, the pharmacological IKK inhibitor BMS-345541 significantly reduced Nlrp3 levels in LPS-primed *A20*$^{myel\text{-}KO}$ macrophages (Fig. 3f). Moreover, both BMS-345541 and the selective IKK2 inhibitor TCPA-1 significantly reduced ATP- and nigericin-induced caspase-1 autoprocessing, IL-1β secretion and pyroptosis induction in LPS-primed *A20*$^{myel\text{-}KO}$ macrophages (Fig. 3g-i).

Having established A20 as a negative regulator of Nlrp3 inflammasome activation, we hypothesized that excessive Nlrp3 activation might drive RA pathology in A20-deficient mice upstream of IL1R1. To test this hypothesis, *Nlrp3*$^{-/-}$ mice were crossed into *A20*$^{myel\text{-}KO}$ mice and the levels of 4 RA-relevant cytokines (IL-1α, IL-1β, IL-6 and TNF) were monitored. Although IL-1α levels were not significantly different in A20-sufficient and *A20*$^{myel\text{-}KO}$ mice (Extended Data figure 4a), the latter mice had significantly higher levels of IL-1β in circulation (Fig. 4a). In addition, the levels of IL-6 and TNF were also significantly higher in *A20*$^{myel\text{-}KO}$ mice compared to *A20*$^{flox/flox}$ littermates (Extended Data figure 4b, c). Notably, deletion of Nlrp3 in *A20*$^{myel\text{-}KO}$ mice markedly reduced IL-1β secretion to baseline levels of *A20*$^{flox/flox}$ mice, thereby demonstrating that the Nlrp3 inflammasome contributes critically to excessive IL-1β production in *A20*$^{myel\text{-}KO}$ mice *in vivo* (Fig. 4a). Intriguingly, *A20*$^{myel\text{-}KO}$*Nlrp3*$^{-/-}$ mice also were protected from excessive IL-6 production, suggesting that high IL-6 levels are consequent to excessive inflammasome-mediated IL-1β production (Extended Data figure 4b). In contrast, TNF production was not significantly affected in *A20*$^{myel\text{-}KO}$*Nlrp3*$^{-/-}$ and *A20*$^{myel\text{-}KO}$*Casp1*$^{-/-}$ mice (Extended Data figure 4c). In agreement, TNF-R1 signaling was previously shown to be dispensable for RA pathology in *A20*$^{myel\text{-}KO}$ mice, whereas IL-6 neutralization provided protection[2].

Based on these findings, we assessed the contribution of Nlrp3 to RA pathogenesis in *A20*$^{myel\text{-}KO}$ mice. Swelling and redness of the hind paws of *A20*$^{myel\text{-}KO}$*Nlrp3*$^{+/+}$ mice became evident around 11 weeks of age (Fig. 4b), and had afflicted all animals of this genotype when they were 20 weeks old (Fig. 4c). Disease severity continued to progress, and became increasingly pronounced in *A20*$^{myel\text{-}KO}$*Nlrp3*$^{+/+}$ mice of 21-40 weeks old (Fig. 4d). In contrast, *A20*$^{myel\text{-}KO}$*Nlrp3*$^{-/-}$mice of similar age were markedly protected from RA, and their hind paws had a normal appearance and lacked clinical signs of RA pathology (Fig. 4b-d). Histological analysis of the ankle joints of these mice showed significantly reduced synovial and periarticular inflammation, and substantially less infiltrated mononuclear cells compared to tissue sections of *A20*$^{myel\text{-}KO}$*Nlrp3*$^{+/+}$ mice of comparable

age (Fig. 4e, f and Extended Data Table 2). In agreement, three-dimensional micro-CT imaging showed that the extent of bone erosion in hind paws of representative *A20*$^{myel\text{-}KO}$*Nlrp3*$^{+/+}$ and *A20*$^{myel\text{-}KO}$*Nlrp3*$^{-/-}$ mice was markedly different. Unlike in Nlrp3-deficient *A20*$^{myel\text{-}KO}$ mice, hind paws of Nlrp3-sufficient mice exhibited severe loss of bone density in the metatarsal region (Fig. 4g), demonstrating a key role for Nlrp3 in RA pathology. We also analyzed the impact of caspase-1/11-deficiency on IL-1β secretion and RA pathology in *A20*$^{myel\text{-}KO}$ mice. IL-1β levels in circulation were significantly reduced in *A20*$^{myel\text{-}KO}$*Casp1/11*$^{-/-}$mice compared to *A20*$^{myel\text{-}KO}$*Casp1/11*$^{+/+}$ and *A20*$^{flox/flox}$ mice (Fig. 4h). As in *A20*$^{myel\text{-}KO}$*Nlrp3*$^{-/-}$mice, serum levels of IL-6 were markedly reduced in *A20*$^{myel\text{-}KO}$*Casp1/11*$^{-/-}$ mice, whereas TNF production was not significantly different compared to *A20*$^{myel\text{-}KO}$*Casp1/11*$^{+/+}$ mice (Extended Data figure 4). Moreover, hind paws of all analyzed *A20*$^{myel\text{-}KO}$*Casp1/11*$^{+/+}$ mice were clearly inflamed and swollen (Fig. 4i-k). In contrast, 50% of *A20*$^{myel\text{-}KO}$*Casp1/11*$^{-/-}$ mice were devoid of clinical signs of arthritis, and disease symptoms in the remaining *A20*$^{myel\text{-}KO}$*Casp1/11*$^{-/-}$ mice were very mild (Fig. 4i-k). In agreement, analysis of heamatoxylin & eosin-stained joint sections of arthritic *A20*$^{myel\text{-}KO}$*Casp1/11*$^{+/-}$ mice showed massive mononuclear cell infiltration associated with marked articular, periarticular and synovial inflammation and reactive fibrosis. In contrast, joints of *A20*$^{myel\text{-}KO}$*Casp1/11*$^{-/-}$ mice were markedly protected from RA histopathology (Fig. 4l).

Collectively, these results demonstrate that A20 puts a brake on Nlrp3 inflammasome activation by reducing basal and LPS-induced Nlrp3 expression levels (Extended Data Fig. 5). Moreover, we showed that excessive Nlrp3 inflammasome activation drives arthritis pathogenesis in *A20*$^{myel\text{-}KO}$ mice. Arthritis in humans is a complex disease that may be caused by different combinations of genetic and environmental triggers. As such, available RA mouse models may each be relevant to distinct subsets of RA patients, or suitable to study certain aspects of RA pathogenesis. Pathology in the widely used collagen- and albumin-induced mouse arthritis models occurs independently of inflammasome signaling[13,14]. In contrast, we demonstrated here that arthritis pathology in *A20*$^{myel\text{-}KO}$ mice critically relies on the Nlrp3 inflammasome/IL-1 signaling axis. Because both *A20/Tnfaip3*[15-18] and *Nlrp3*[19-21] are RA-susceptibility genes, this suggests that *A20*$^{myel\text{-}KO}$ mice might be a suitable pre-clinical model for validating the effectiveness of experimental RA therapies targeting inflammasomes and/or IL-1 signaling.

Methods

Mice

A20$^{myel\text{-}KO}$ mice with a lysosome M-Cre-targeted deletion of A20 in myeloid cells were described[2]. *Nlrp3*$^{-/-}$[22] and Casp1$^{-/-}$[23] mice have been described, and were kindly provided by Dr. V. Dixit (Genentech) and Dr. R. Flavell (Yale University). IL1R1$^{-/-}$[24] mice were purchased from Jackson Laboratories and bred in-house. *In vivo* experiments were controlled with age- and sex-matched littermates. The sample size was chosen so as to validate statistical analyses. Mice were housed in individually ventilated cages and kept under pathogen-free conditions at animal facilities of Ghent University. All animal

experiments were conducted with permission of the Ethical committees on laboratory animal welfare of Ghent University.

Macrophage differentiation and stimulation

Bone marrow-derived macrophages (BMDMs) were generated by culturing bone marrow cells in IMDM containing 10% heat-inactivated FBS, 30% L cell-conditioned medium, 100 U ml^{-1} penicillin, and 100 mg ml^{-1} streptomycin at 37°C in a humidified atmosphere containing 5% CO_2. 6 days later, cells were collected and seeded in 12-well plates in IMDM containing 10% heat-inactivated FBS and 1% non-essential amino acids in the presence of antibiotics. The next day BMDMs were either left untreated or treated with 5 μg ml^{-1} ultrapure LPS from *Salmonella minnesota* (Invivogen) for 3 h followed by 5 mM ATP (Roche) or 20 μM nigericin (Sigma-Aldrich) for 30 min or 0.5 mg ml^{-1} Silica (Min-U-Sil 5, US Silica) for 6 h. BMDMs were also separately infected with *Salmonella enterica* serovar Typhimurium at the indicated multiplicity of infection (MOI) for 3 h, the last hour of which in the presence of gentamycin (50 μg ml^{-1}). To activate the AIM2 inflammasome, BMDMs were left untreated or treated with 5 μg ml^{-1} LPS for 3 h. After removal of LPS, BMDMs were exposed to Lipofectamine 2000 (mock, Life Technologies) or Lipofectamine with 1.25 ug ml^{-1} pCDNA3 plasmid DNA for 19 h. To induce rapid Nlrp3 inflammasome activation, BMDMs were stimulated with LPS for 10 min, and then treated with ATP or nigericin for 45 min. For inhibition of NF-κB, $A20^{myel\text{-}KO}$ BMDMs were preincubated for 30 min with 1.25 or 2.5 μM of the selective IKK inhibitors BMS-345541[25] or TPCA-1[26] (Sigma-Aldrich) before stimulation with LPS.

Western blotting

Cell lysates and culture supernatants were incubated with cell lysis buffer (20 mM Tris HCl pH 7.4, 200 mM NaCl, 1% NP-40) and denatured in laemmli buffer. Subsequently the protein samples were boiled at 95°C for 10 min and separated by SDS-PAGE. Separated proteins were transferred to PVDF membranes. Blocking, incubation with antibody and washing of the membrane were done in PBS supplemented with 0.05% Tween-20 (v/v) and 3% (w/v) non-fat dry milk. Immunoblots were incubated overnight with primary antibodies against caspase-1 (AG-20B-0042-C100, Adipogen), Nlrp3 (AG-20B-0014-C100, Adipogen), ASC (AG-25B-0006, Adipogen), IL-1β (GTX74034, Genetex), IL-18 (5180R-100, Biovision), IkBα (9242S, Cell Signaling), Phospho-IkBα (2859S, Ser32) (Cell Signaling), β-actin (NB600-501H, Novus Biologicals) and A20 (sc-166692, Santa Cruz Biotechnology). Horseradish peroxidase-conjugated goat anti-mouse (115-035-146, Jackson Immunoresearch Laboratories) or anti-rabbit secondary antibody (111-035-144, Jackson Immunoresearch Laboratories) was used to detect proteins by enhanced chemiluminescence (Thermo Scientific).

Cytokine analysis and LDH measurement

Cytokine levels in culture medium and serum were determined by magnetic bead-based multiplex assay using Luminex technology (Bio-Rad) and IL1β ELISA (R&D Systems), according to the manufacturers' instructions. Cell death levels were determined by LDH assay in culture medium according to the manufacturer's instructions (Promega).

RT-PCR

Total RNA was isolated from BMDMs using RNeasy kit (Qiagen). cDNA was synthesized using the QuantiTect Reverse Transcription Kit (Qiagen). A20 mRNA expression in wild-type and A20$^{myel\text{-}KO}$ BMDMs, treated with 5 μg ml^{-1} LPS for 6 h, was determined by RT-PCR using the following primers: 5′-CTCGGAACTTTAAATTCCGC-3′ and 5′-GGGTAAGTTAGCTTCATCC-3′. To analyse mRNA levels of Nlrp3, proIL-1β, ASC and caspase-1, wild-type and A20$^{myel\text{-}KO}$ BMDMs were left untreated or treated with 5 μg ml^{-1} LPS for 3 h and Quantitative RT-PCR (qRT-PCR) was performed using LightCycler 480 SYBR Green I Master Mix Kit (Roche Applied Science) in a LightCycler 480 real-time PCR machine (Roche Applied Science). The cycling conditions were 95°C for 5 min followed by 45 cycles of 95°C for 10 s, 60°C for 15 s, and 72°C for 20 s. Gene expression levels were normalized to GAPDH. qRT-PCR Sense/antisense primers used: Mouse GAPDH, 5′-GGTGAAGGTCGGTGTGAACG-3′ and 5′-CTCGCTCCTGGAAGATGGTG-3′; Mouse Nlrp3, 5′-ATTACCCGCCCGAGAAAGG-3′ and 5′-TCGCAGCAAAGATCCACACAG-3′; Mouse proIL-1β, 5′-TGGGCCTCAAAGGAAAGA-3′ and 5′-GGTGCTGATGTACCAGTT-3′; Mouse ASC, 5′-CTTGTCAGGGGATGAACTCAAAA-3′ and 5′-GCCATACGACTCCAGATAGTAGC-3′; Mouse Casp1, 5′-ACAAGGCACGGGACCTATG-3′ and 5′-TCCCAGTCAGTCCTGGAAATG-3′. Quantitative analysis of mouse proIL-18 mRNA was performed using Taqman gene expression assay (Mm00434225_m1, Applied Biosystems).

Clinical scoring

Mice were randomly scored in a blinded fashion for development of peripheral arthritis once a week and scores were subsequently linked to genotypes. A score ranging from 0 to 3 was assigned to each paw, with 0 being normal, 0.5 being swelling of one or more toes, 1 being mild swelling of the wrist and/or ankle or carpus and/or tarsus, 2 being moderate swelling of the wrist and/or ankle or carpus and/or tarsus or mild swelling of both, and 3 being severe swelling of the entire paw.

Micro-CT Imaging

Micro-CT micrographs of paws fixed in formalin were made using an ex vivo micro-CT scanner (LocusSP Specimen CT, GE Healthcare) at 28-μm isotropic voxel size, with 720 projections, an integration time of 1,700 msec, photon energy of 80 keV, and a current of 70 μA.

Histology and histological scoring

Murine paws were dissected, fixed in 4% formaldehyde, decalcified in 5% formic acid until bones were pliable. Paraffin sections were stained with H&E for evaluation of inflammation and bone erosions. Histological sections were evaluated by two blinded assessors, and scores were determined by combining assessment of 2 parameters, calcaneal erosion and inflammation at the synovio-entheseal complex, each ranging from 0 (normal) to 3. (erosion: 0 none, 1 minimal, 2 intermediate, 3 into bone marrow; Inflammation: 0 none, 1: minimal 1-2 cell layers, 2: 2-5 cell layers, 3: >5 cell layers).

Europe PMC Funders Author Manuscripts

Statistics

GraphPad Prism 5.0 software was used for data analysis. Data are shown as mean with standard deviation (s.d.). Data were compared by an unpaired 2-tailed Student's t-test when values followed a Gaussian distribution, or with the non-parametric Mann-Whitney U test. $P < 0.05$ was considered to indicate statistical significance.

Supplementary Material

Refer to Web version on PubMed Central for supplementary material.

Acknowledgements

We thank Richard Flavell (Yale University) and Vishva Dixit (Genentech) for generous supply of mutant mice. LVW is a postdoctoral fellow with the Fund for Scientific Research-Flanders. This work was supported by the Ghent University Concerted Research Actions (grant BOF14/GOA/013) and grants from the European Research Council (Grant 281600) and the Fund for Scientific Research (FWO)-Flanders (grants G030212N, 1.2.201.10.N.00 and 1.5.122.11.N.00) to M.L., and by FWO research grants (Odysseus-G091908, G061910N and G016812N) and the Ghent University 'Group-ID MRP' to G.V.L., R.B. and D.E. T-D.K is supported by grants from the National Institute of Health (Grants AR056296, CA163507 and AI101935) and the American Lebanese Syrian Associated Charities (ALSAC).

Abbreviations

RA	rheumatoid arthritis
TNFAIP3	Tumor necrosis factor, alpha-induced protein 3
caspase	cysteinyl aspartate-specific protease
NLR	NOD-like receptor
IL1R1	Interleukin 1 receptor, type I
wt	wild-type

References

1. Burger D, Dayer JM, Palmer G, Gabay C. Is IL-1 a good therapeutic target in the treatment of arthritis? Best Pract Res Clin Rheumatol. 2006; 20:879–896. [PubMed: 16980212]
2. Matmati M, et al. A20 (TNFAIP3) deficiency in myeloid cells triggers erosive polyarthritis resembling rheumatoid arthritis. Nat Genet. 2011; 43:908–912. [PubMed: 21841782]
3. Lamkanfi M, Dixit VM. Inflammasomes and their roles in health and disease. Annu Rev Cell Dev Biol. 2012; 28:137–161. [PubMed: 22974247]
4. Bauernfeind FG, et al. Cutting edge: NF-kappaB activating pattern recognition and cytokine receptors license NLRP3 inflammasome activation by regulating NLRP3 expression. J Immunol. 2009; 183:787–791. [PubMed: 19570822]
5. Wertz IE, et al. De-ubiquitination and ubiquitin ligase domains of A20 downregulate NF-kappaB signalling. Nature. 2004; 430:694–699. [PubMed: 15258597]
6. Vereecke L, Beyaert R, van Loo G. The ubiquitin-editing enzyme A20 (TNFAIP3) is a central regulator of immunopathology. Trends Immunol. 2009; 30:383–391. [PubMed: 19643665]
7. Lee EG, et al. Failure to regulate TNF-induced NF-kappaB and cell death responses in A20-deficient mice. Science. 2000; 289:2350–2354. [PubMed: 11009421]
8. Boone DL, et al. The ubiquitin-modifying enzyme A20 is required for termination of Toll-like receptor responses. Nat Immunol. 2004; 5:1052–1060. [PubMed: 15334086]

9. Fernandes-Alnemri T, et al. Cutting edge: TLR signaling licenses IRAK1 for rapid activation of the NLRP3 inflammasome. J Immunol. 2013; 191:3995–3999. [PubMed: 24043892]
10. Juliana C, et al. Non-transcriptional priming and deubiquitination regulate NLRP3 inflammasome activation. J Biol Chem. 2012; 287:36617–36622. [PubMed: 22948162]
11. Lin KM, et al. IRAK-1 bypasses priming and directly links TLRs to rapid NLRP3 inflammasome activation. Proc Natl Acad Sci U S A. 2014; 111:775–780. [PubMed: 24379360]
12. Schroder K, et al. Acute lipopolysaccharide priming boosts inflammasome activation independently of inflammasome sensor induction. Immunobiology. 2012; 217:1325–1329. [PubMed: 22898390]
13. Ippagunta SK, et al. Inflammasome-independent role of apoptosis-associated speck-like protein containing a CARD (ASC) in T cell priming is critical for collagen-induced arthritis. J Biol Chem. 2010; 285:12454–12462. [PubMed: 20177071]
14. Kolly L, et al. Inflammatory role of ASC in antigen-induced arthritis is independent of caspase-1, NALP-3, and IPAF. J Immunol. 2009; 183:4003–4012. [PubMed: 19717512]
15. Wellcome Trust Case Control Consortium. Genome-wide association study of 14,000 cases of seven common diseases and 3,000 shared controls. Nature. 2007; 447:661–678. [PubMed: 17554300]
16. Dieguez-Gonzalez R, et al. Analysis of TNFAIP3, a feedback inhibitor of nuclear factor-kappaB and the neighbor intergenic 6q23 region in rheumatoid arthritis susceptibility. Arthritis Res Ther. 2009; 11:R42. [PubMed: 19292917]
17. Plenge RM, et al. Two independent alleles at 6q23 associated with risk of rheumatoid arthritis. Nat Genet. 2007; 39:1477–1482. [PubMed: 17982456]
18. Thomson W, et al. Rheumatoid arthritis association at 6q23. Nat Genet. 2007; 39:1431–1433. [PubMed: 17982455]
19. Ben Hamad M, et al. Association study of CARD8 (p.C10X) and NLRP3 (p.Q705K) variants with rheumatoid arthritis in French and Tunisian populations. Int J Immunogenet. 2012; 39:131–136. [PubMed: 22128899]
20. Kastbom A, et al. Genetic variation in proteins of the cryopyrin inflammasome influences susceptibility and severity of rheumatoid arthritis (the Swedish TIRA project). Rheumatology. 2008; 47:415–417. [PubMed: 18263599]
21. Mathews RJ, et al. Evidence of NLRP3-inflammasome activation in rheumatoid arthritis (RA); genetic variants within the NLRP3-inflammasome complex in relation to susceptibility to RA and response to anti-TNF treatment. Ann Rheum Dis. 2013
22. Mariathasan S, et al. Cryopyrin activates the inflammasome in response to toxins and ATP. Nature. 2006; 440:228–232. [PubMed: 16407890]
23. Schott WH, et al. Caspase-1 is not required for type 1 diabetes in the NOD mouse. Diabetes. 2004; 53:99–104. [PubMed: 14693703]
24. Glaccum MB, et al. Phenotypic and functional characterization of mice that lack the type I receptor for IL-1. J Immunol. 1997; 159:3364–3371. [PubMed: 9317135]
25. Burke JR, et al. BMS-345541 is a highly selective inhibitor of I kappa B kinase that binds at an allosteric site of the enzyme and blocks NF-kappa B-dependent transcription in mice. J Biol Chem. 2003; 278:1450–1456. [PubMed: 12403772]
26. Podolin PL, et al. Attenuation of murine collagen-induced arthritis by a novel, potent, selective small molecule inhibitor of IkappaB Kinase 2, TPCA-1 (2-[(aminocarbonyl)amino]-5-(4-fluorophenyl)-3-thiophenecarboxamide), occurs via reduction of proinflammatory cytokines and antigen-induced T cell Proliferation. J Pharmacol Exp Ther. 2005; 312:373–381. [PubMed: 15316093]

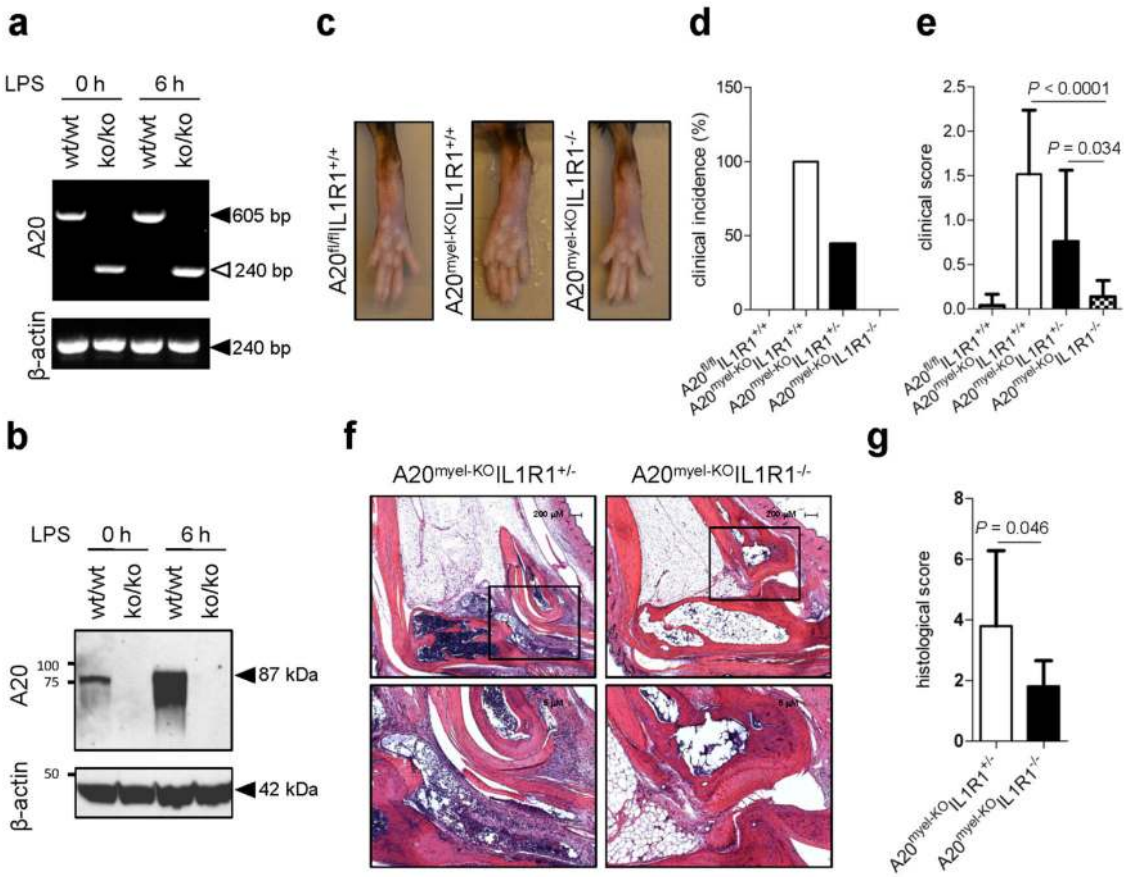

Figure 1. Il1r1-deficiency rescues the arthritis phenotype of A20$^{myel\text{-}KO}$ mice

a, b, A20 and β-actin mRNA (a) and protein (b) levels of LPS-stimulated BMDMs. **c,** Hind paws of 20 weeks old mice. **d, e,** A20$^{fl/fl}$IL1R1$^{+/+}$ (n=19), A20$^{myel\text{-}KO}$IL1R1$^{+/+}$ (n=8), A20$^{myel\text{-}KO}$IL1R1$^{+/-}$ (n=15) and A20$^{myel\text{-}KO}$IL1R1$^{-/-}$ (n=9) mice aged 21-30 weeks were clinically scored for arthritis incidence (d) and severity (e). **f,** Ankle joints sections stained with haematoxylin and eosin; magnification: 40× (top) and 100x (bottom). **g,** Histological scores of ankle sections of A20$^{myel\text{-}KO}$IL1R1$^{+/-}$ (n=10) and A20$^{myel\text{-}KO}$IL1R1$^{-/-}$ (n=8). *P*-values in **e** and **g** were determined by Student's t-test.

Europe PMC Funders Author Manuscripts

Europe PMC Funders Author Manuscripts

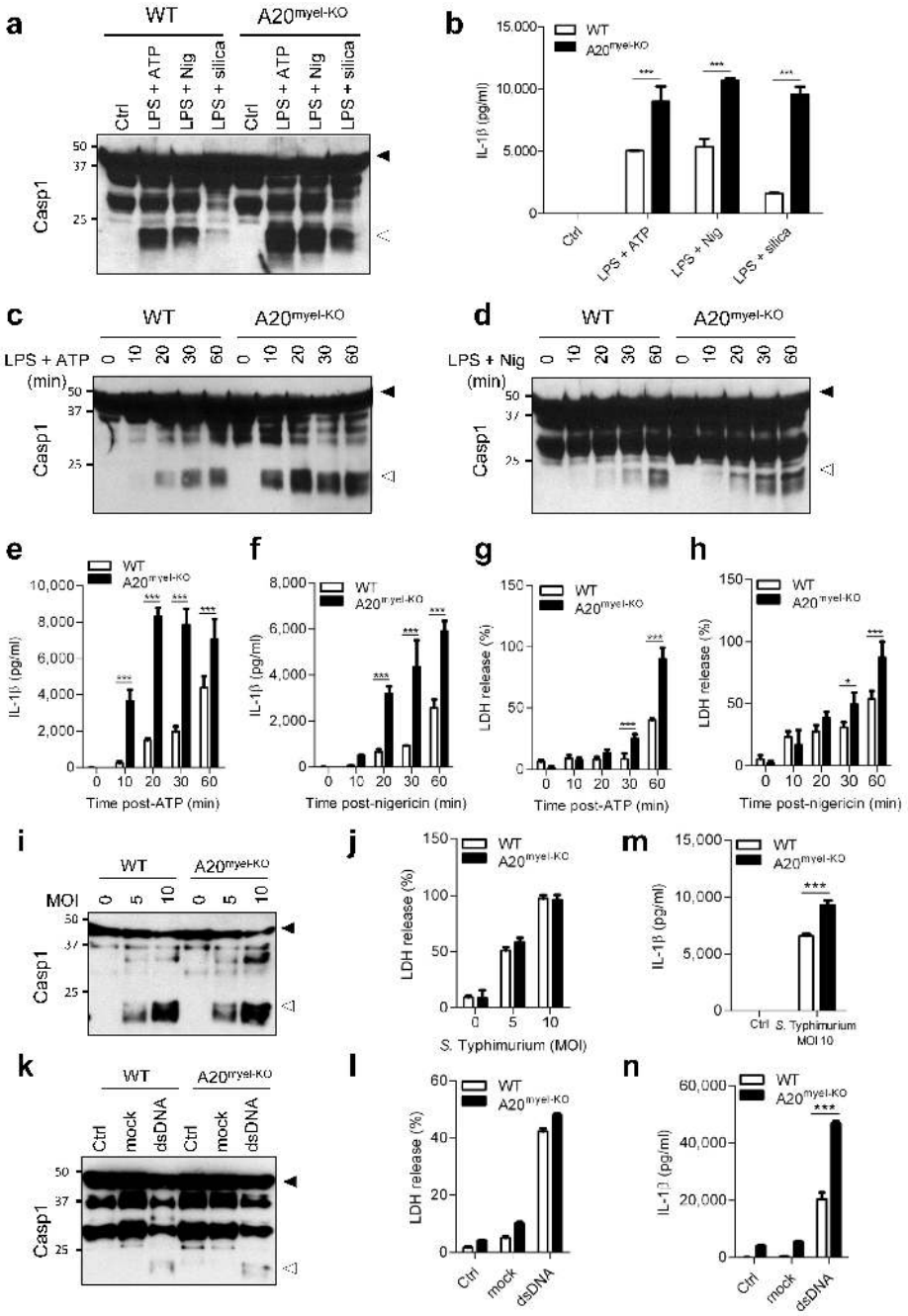

Figure 2. Hyperactivation of the Nlrp3, but not the Nlrc4 and AIM2 inflammasomes, in A20-deficient macrophages

a-h, BMDMs were stimulated as described in Methods. Lysates were immunoblotted for caspase-1 (a, c, d) and supernatants analyzed for IL-1β (b, e, f) and LDH (g, h). **i-n,** BMDMs were treated as described in Methods. Lysates were immunoblotted for caspase-1 (i, k) and supernatants analyzed for LDH (j, l) and IL-1β (m, n). Black arrow, procaspase-1; white arrow, p20. Data represent mean ± s.d. of 1 out of 3 biological replicates, with 3 technical replicates each (*$P < 0.05$; ***$P < 0.001$; Student's t-test).

Europe PMC Funders Author Manuscripts

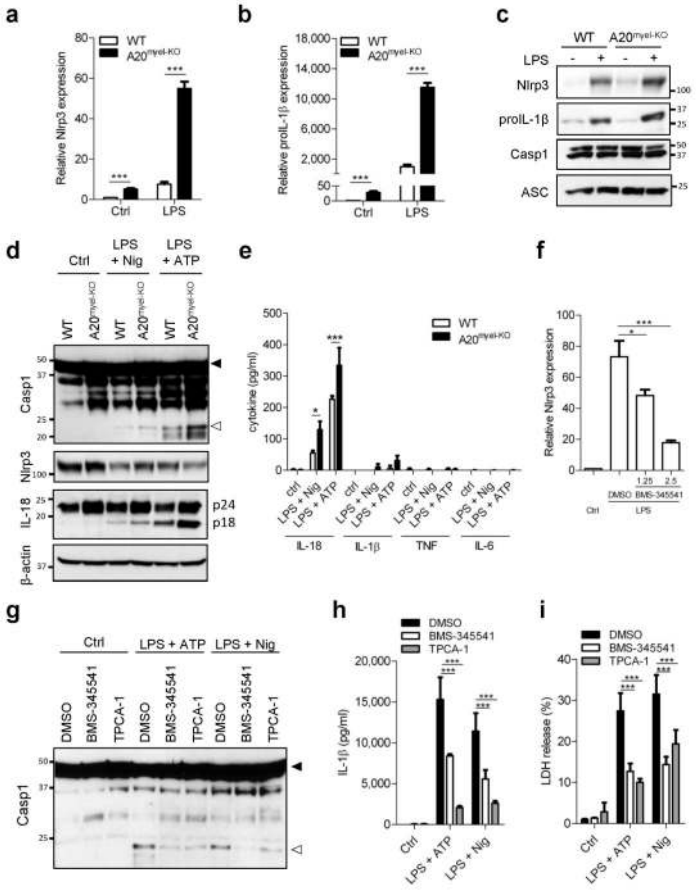

Figure 3. A20 inhibits Nlrp3 inflammasome priming

a, b, Nlrp3 (a) and proIL-1β (b) mRNA levels of LPS-treated BMDMs. **c,** Expression of the indicated proteins in BMDMs 6 h after LPS treatment. **d, e,** Rapid Nlrp3 inflammasome activation as described in Methods. Expression of the indicated proteins (d), and secreted cytokines (e) were determined. **f-i,** A20$^{myel\text{-}KO}$ BMDMs were treated as indicated. Nlrp3 mRNA levels (f), caspase-1 expression (g), secreted IL-1β (h) and LDH activity (i) were determined. Black arrow, procaspase-1; white arrow, p20. Data represent mean ± s.d. of 1 out of 3 biological replicates, with 3 technical replicates each (*P < 0.05; ***P < 0.001; Student's t-test).

Europe PMC Funders Author Manuscripts

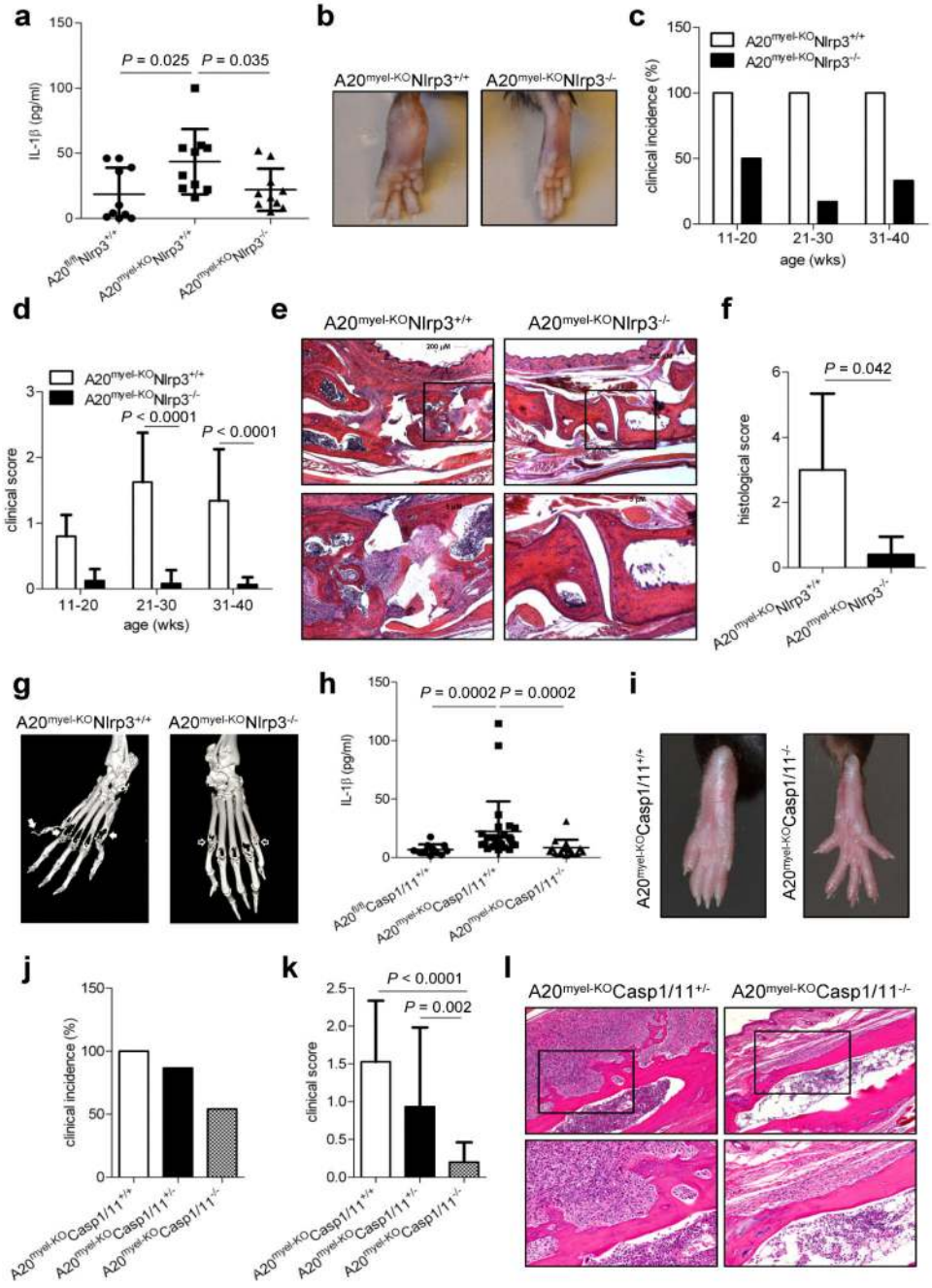

Figure 4. Nlrp3 and caspase-1 deletion rescues arthritis in A20$^{myel\text{-}KO}$ mice

a, IL1β serum levels of A20$^{fl/fl}$Nlrp3$^{+/+}$ (n=10), A20$^{myel\text{-}KO}$Nlrp3$^{+/+}$ (n=10) and A20$^{myel\text{-}KO}$Nlrp3$^{-/-}$ (n=10) mice aged 20-35 weeks. **b,** Hind paws of 30 weeks old mice. **c, d,** A20$^{myel\text{-}KO}$Nlrp3$^{+/+}$ (n = 20) and A20$^{myel\text{-}KO}$Nlrp3$^{-/-}$(n=17) mice were scored for arthritis incidence (d) and severity (e). **e,** Representative ankle joints sections; magnification: 40× (top) and 100x (bottom). **f,** Histological scores of ankle sections of A20$^{myel\text{-}KO}$Nlrp3$^{+/+}$ (n=5) and A20$^{myel\text{-}KO}$Nlrp3$^{-/-}$ (n=5) mice. **g,** micro-CT images of hind paws of A20$^{myel\text{-}KO}$Nlrp3$^{+/+}$ and A20$^{myel\text{-}KO}$Nlrp3$^{-/-}$ mice. Solid arrow, bone erosion; empty

arrow, intact cartilage and bone. **h,** IL-1β serum levels of $A20^{fl/fl}Casp1/11^{+/+}$ (n=11), $A20^{myel\text{-}KO}Casp1/11^{+/+}$ (n=26) and $A20^{myel\text{-}KO}Casp1/11^{-/-}$ (n=16) mice aged 20-35 weeks. **i,** Hind paws of 25 weeks old mice. **j, k,** 15-30 weeks old $A20^{myel\text{-}KO}Casp1/11^{+/+}$ (n=12), $A20^{myel\text{-}KO}Casp1/11^{+/-}$(n=15) and $A20^{myel\text{-}KO}Casp1/11^{-/-}$ (n=24) mice were clinically scored for arthritis incidence (j) and severity (k). **l,** Representative ankle joints sections; magnification: 40× (top) and 100x (bottom). *P*-values were determined by Student's t-test (a, d, f, k) and Mann-Whitney test (h).

Europe PMC Funders Author Manuscripts